An Investigation of Sensitivity of Vector Controlled DFIG to Rotor Position and Machine Parameter Measurement Errors

Kennedy Adinbo Aganah, Member, IEEE

Department of Electrical Engineering
Tuskegee University, Tuskegee Institute, USA
Email: adinbo@ieee.org

Abstract: This paper investigates the effects of rotor position error and machine parameter inaccuracies on a vector-controlled DFIG turbine system. A detailed modeling of the errors has been provided and simulation results show that the error in rotor position has a significant effect on the performance and stability of the entire system. It has been established that for properly tuned PI controller gains, the machine parameter mismatches do not affect the stability of the system even though they mildly affect the placement of the system poles in the left-hand plane.

Keywords: DFIG, vector control, measurement errors, parameter sensitivity.

I. INTRODUCTION

Doubly-Fed Induction Generators (DFIGs) are widely used in wind turbine power applications. They are comparatively cheaper since the converters are not rated at full turbine power. The common control schemes used to control the flow of active and reactive powers to and from the grid include Direct Power and Direct Torque controls [1]-[3], and Vector control [4]-[6]. The former have the advantage of having a simpler structure and less dependence on machine parameters. The drawback of the Direct Torque control is that it requires variable switching frequency.

In the vector control schemes, decoupling of active and reactive powers is usually achieved by aligning the d-axis on either the stator flux vector position [5], [6] or the stator voltage vector position [4]. Fig. 1 shows a typical vector control scheme utilizing coordinate transformations which heavily rely on accurate knowledge of the rotor position as well as stator flux/voltage angle. Therefore, any error in angle measurements/estimates will result in inaccurate reference signals (voltages, currents, speed and power).

Reference [5] investigates the effects of errors in slip angle while [6] and [7] examine the sensitivity of the vector control scheme system to errors in estimating machine parameters such as the stator, rotor and mutual inductances as well as the rotor position error [6] in a sensorless model. This paper analyzes the combined effect of the inaccuracies in machine inductances and rotor position for the control system shown in Fig. 1.

The symbols used here are defined below:

$\hat{}, *$: observed and reference variables

$v_{qs}, v_{ds}\ v_{qr}, v_{dr}$: Stator and rotor $q-d$ voltages

$i_{qs}, i_{ds}, i_{qr}, i_{dr}$: Stator and rotor $q-d$ currents

$a_{qs}, a_{ds}\ a_{qr}, a_{dr}$: Stator and rotor $q-d$ flux linkages

μ_e, μ_r : Stator reference and rotor angular speeds

θ_e, θ_r : Stator reference and rotor angles

$\theta_{sr} = \theta_s - \theta_r$: Slip angle

$\Delta\theta_{sr} = \hat{\theta}_{sr} - \theta_{sr}$: Error in slip angle

$\mu_{sr} = \mu_e - \mu_r$: Slip speed

L_s, L_r, L_m : Stator, rotor and mutual inductances

$\sigma = 1 - L_m^2 / L_s L_s$: Leakage inductance

$e_{\mu_{sr}} = \hat{\mu}_{sr} / \mu_{sr}, \quad e_{L_r} = \hat{L}_r / L_r, \quad e_{\sigma} = \hat{\sigma} / \sigma, \quad e_{L_s} = \hat{L}_s / L_s$

T_e, T_m : Electromagnetic and turbine torques

P, J : Number of poles and inertia of combined turbine-generator system and $p = d/dt$: time derivative

$k_p^c, k_p^\mu, k_p^q, and\ k_i^c, k_i^\mu, k_i^q$: Proportional and integral gains of current, speed and reactive power controllers.

II. MODELING THE EFFECTS OF ERRORS

A. Inner Current Control Loop

The $q-d$ axes current controller can be modeled as:

$$\left.\begin{aligned} px_1^c &= i_{qr}^* - \hat{i}_{qr} \\ px_2^c &= i_{dr}^* - \hat{i}_{dr} \end{aligned}\right\} \tag{1}$$

$$\left.\begin{aligned} v_{qr}^* &= \left(k_{p1}^c + \frac{k_{i1}^c}{p}\right)\left(i_{qr}^* - \hat{i}_{qr}\right) \\ v_{dr}^* &= \left(k_{p2}^c + \frac{k_{i2}^c}{p}\right)\left(i_{dr}^* - \hat{i}_{dr}\right) \end{aligned}\right\} \tag{2}$$

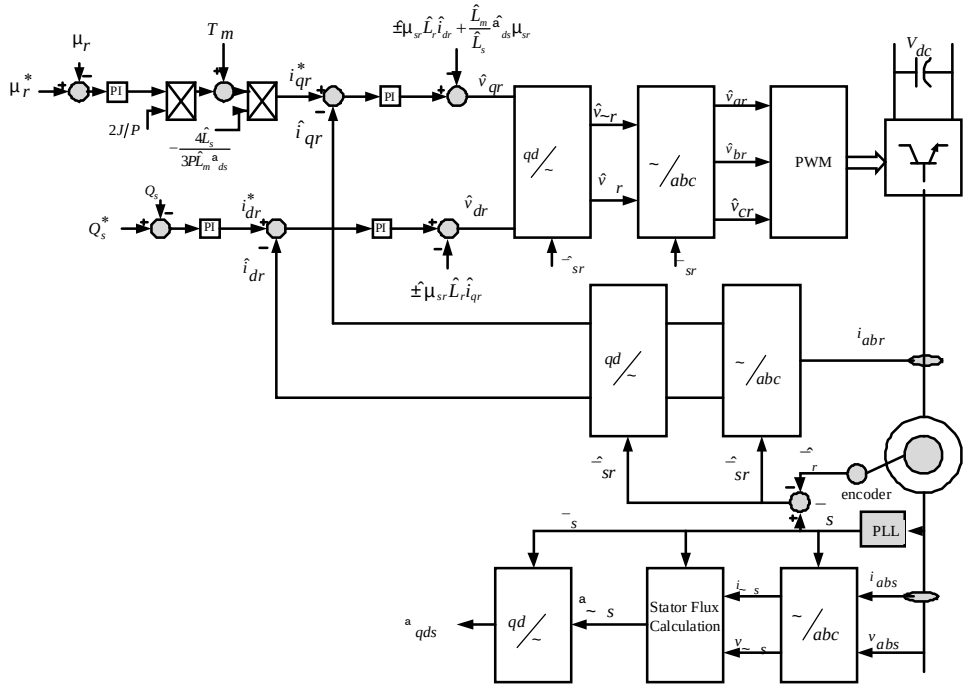

Figure. 1: Rotor-side Converter Control Structure

It can be shown that the observed rotor voltage equations are given by:

$$\left.\begin{aligned}\hat{v}_{qr} &= k_p i_{qr}^* - k_p \hat{i}_{qr} + k_{i1}^c x_1^c + \pm\hat{\mu}_{sr}\hat{L}_r i_{dr} + \frac{\hat{L}_m}{\hat{L}_s}\hat{a}_{ds}\hat{\mu}_{sr}\\ \hat{v}_{dr} &= k_{p2}^c i_{dr}^* - k_{p2}^c \hat{i}_{dr} + k_{i2}^c x_2^c - \hat{\mu}_{sr}\pm\hat{L}_r i_{qr}\end{aligned}\right\} \quad (3)$$

Combining (1) and (3), a fourth-order dynamic system can be obtained as in (4).

$$px = A^c x + B^c u + E^c \quad (4)$$

where $x = \begin{bmatrix}\hat{i}_{qr} & \hat{i}_{dr} & x_1^c & x_2^c\end{bmatrix}^T$, $u = \begin{bmatrix}i_{qr}^* & i_{dr}^*\end{bmatrix}^T$ and the system matrix is given by (5).

$$A^c = \begin{bmatrix} -\dfrac{r_r + k_p^c}{\pm L_r} & -\mu_{sr} + \dfrac{\pm\hat{\mu}_{sr}\hat{L}_r}{\pm L_r} & \dfrac{1}{\pm L_r}k_i^c & 0 \\ \mu_{sr} - \dfrac{\pm\hat{\mu}_{sr}\hat{L}_r}{\pm L_r} & -\dfrac{r_r + k_p^c}{\pm L_r} & 0 & \dfrac{1}{\pm L_r}k_i^c \\ -1 & 0 & 0 & 0 \\ 0 & -1 & 0 & 0 \end{bmatrix}. \quad (5)$$

An important observation of the system matrix A^c is that it does not contain any slip angle terms. Therefore the stability of the current controller is unaffected by error in rotor position.

B. Stability Analysis

Using the Routh-Hurwitz criteria for a fourth order polynomial, we can establish the conditions for system stability can be established. The Characteristic equation is given by:

$$D(s) = a_4 s^4 + a_3 s^3 + a_2 s^2 + a_1 s + a_0 \quad (6)$$

where $a_0 = \left(k_i^c / \pm L_r\right)^2$,

$$a_1 = \left(2r_r k_i^c + 2k_i^c k_p^c\right) / \pm^2 L_r^2 ,$$

.

$$a_2 = \frac{1}{\pm^2 L_r^2}\begin{pmatrix} 2r_r k_p^c + 2\pm L_r k_i^c + \mu_{sr}^2 \pm^2 L_r^2 + \hat{\mu}_{sr}^2 \pm^2 \hat{L}_r^2 \\ -2\mu_{sr}\pm L_r \hat{\mu}_{sr}\pm\hat{L}_r + \left(k_p^c\right)^2 + r_r^2 \end{pmatrix}$$

$a_3 = 2\left(r_r + k_p^c\right)/\pm Lr$, and $a_4 = 1$.

From the coefficients of the characteristic equation (6), a_4, a_3, a_1, and a_0 are obviously all positive provided the controller gains are positive. However, the coefficient a_2 needs a little more investigation to establish its range. From the contour plot of a_2 shown in Fig. 2, it is safe to say that for properly tuned controller gains, the stability of the current loop is robust to the errors in rotor position and machine parameters. The plots in Fig. 3 confirm this conclusion. The real parts of the eigenvalues are fairly rooted far away from the imaginary axis.

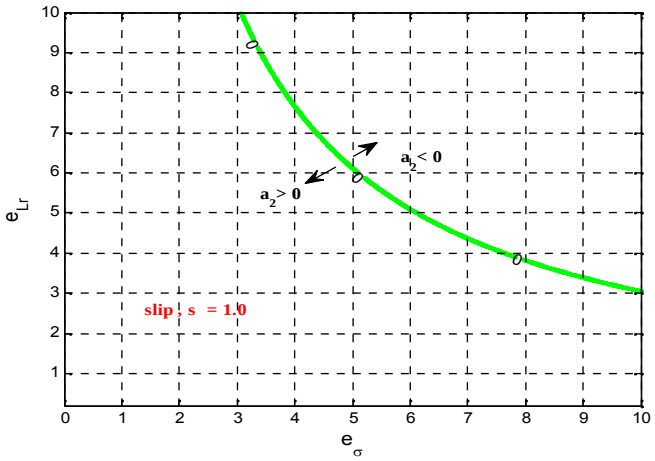

(a)

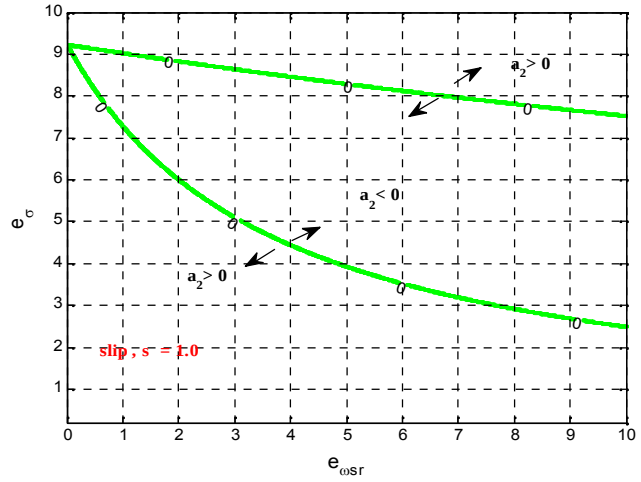

(b)

Figure 2: Contour plot for $a_2 = 0$: (a) variation of the rotor inductance vs. leakage inductance, and (b) variation of the leakage inductance vs. slip speed

C. System Matrix of Speed and Power Loop

The state equations of the rotor speed and reactive power controllers can be written as:

$$px_1^{\mu} = z^* - \hat{z} \tag{7}$$

$$px_2^{q} = Q_s^* - \hat{Q}_s \tag{8}$$

$$i_{qr}^* = \left(k_p^{\mu} + \frac{k_i^{\mu}}{p}\right)\left(z^* - \hat{z}\right) \tag{9}$$

$$i_{dr}^* = \left(k_p^{q} + \frac{k_i^{q}}{p}\right)\left(Q_s^* - \hat{Q}_s\right) \tag{10}$$

The observed rotor angular speed z and stator reactive power are given by (10) and (11) respectively.

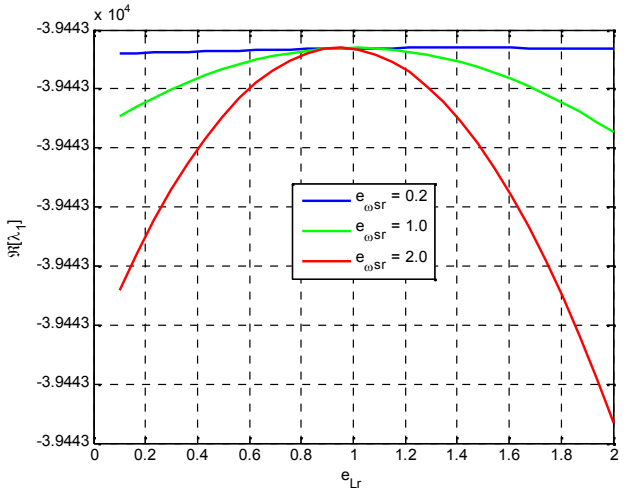

(a)

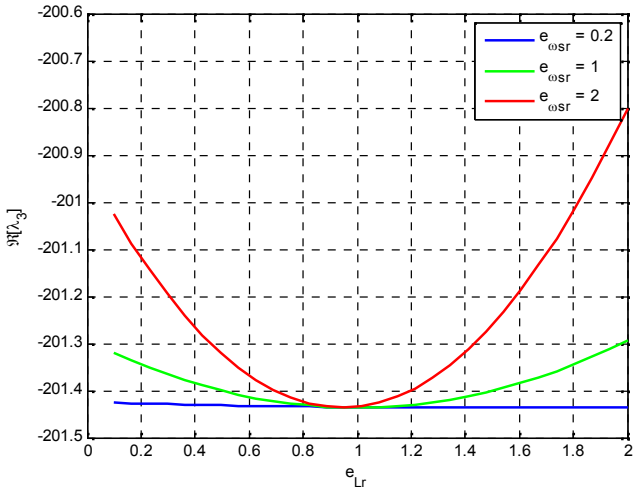

(b)

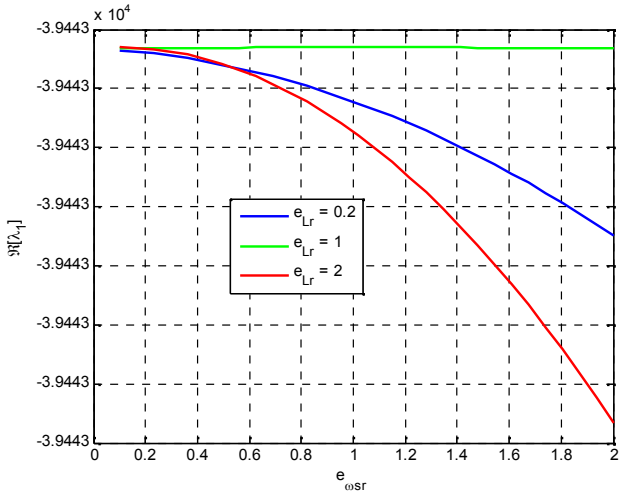

(c)

Figure 3: Contour lines of the real part of the eigenvalues as parameters are varied: (a) $a_{1,2}$ vs rotor inductance, (b) $a_{3,4}$ vs rotor inductance, and (c) $a_{1,2}$ vs rotor slip speed.

$$\hat{z} = -\frac{P}{2J}\left(\frac{3}{2}\frac{P}{2}\frac{\hat{L}_m}{\hat{L}_s}\hat{a}_{ds}T^{-1}\hat{i}_{qr} + T_m\right) \quad (11)$$

$$\hat{Q}_s = \frac{3}{2}\frac{1}{\hat{L}_s}v_s\hat{a}_{ds} - \frac{3}{2}\frac{\hat{L}_m}{\hat{L}_s}v_sT^{-1}\hat{i}_{dr} \quad (12)$$

where T is the $\alpha\beta$ to qd transformation block given by: $T = \begin{bmatrix} \cos\bar{\Delta}_{sr} & \sin\bar{\Delta}_{sr} \\ -\sin\bar{\Delta}_{sr} & \cos\bar{\Delta}_{sr} \end{bmatrix}$.

Substituting (11) and (12) into (7), (8), (9), and (10):

$$px_1^{\mu} = z^* + \frac{P}{2J}\left(\frac{3}{2}\frac{P}{2}\frac{\hat{L}_m}{\hat{L}_s}\hat{a}_{ds}T^{-1}\hat{i}_{qr} + T_m\right) \quad (13)$$

$$px_2^{q} = Q_s^* - \frac{3}{2}\frac{1}{L_s}v_s\hat{a}_{ds} + \frac{3}{2}\frac{\hat{L}_m}{\hat{L}_s}v_sT^{-1}\hat{i}_{dr} \quad (14)$$

$$i_{qr}^* = k_i^{\mu}x_1^{\mu} + k_p^{\mu}\frac{P}{2J}\left(\frac{3}{2}\frac{P}{2}\frac{\hat{L}_m}{\hat{L}_s}\hat{a}_{ds}T^{-1}\hat{i}_{qr} + T_m\right) + k_p^{\mu}z^* \quad (15)$$

$$i_{dr}^* = k_i^{q}x_2^{q} - k_p^{q}\left(\frac{3}{2}\frac{1}{L_s}v_s\hat{a}_{ds} - \frac{3}{2}\frac{\hat{L}_m}{\hat{L}_s}v_sT^{-1}\hat{i}_{dr}\right) + k_p^{q}Q_s^* \quad (16)$$

After some mathematical manipulations, the combined inner current and outer power/speed controllers, a sixth order system is obtained with a system matrix given by (17).

$$A^p = \begin{bmatrix} a & b & \mathrm{m} & 0 & \mathrm{n} & 0 \\ c & d & 0 & m & 0 & n \\ e & f & 0 & 0 & k_i^{\mu} & 0 \\ g & h & 0 & 0 & 0 & k_i^{q} \\ i & j & 0 & 0 & 0 & 0 \\ k & l & 0 & 0 & 0 & 0 \end{bmatrix} \quad (17)$$

In (17), the parameters *a* to *n* are:

$$a = -\frac{r_r + k_p^c}{\sigma L_r} - \frac{3P^2}{8J}\frac{k_p^c k_p^{\omega}}{\sigma L_r}\frac{\hat{L}_m}{\hat{L}_s}\lambda_{ds}\cos(\Delta\theta_{sr}),$$

$$b = \mu_{sr} - \frac{\hat{\mu}_{sr}\pm\hat{L}_r}{\pm\mathrm{L_r}} - \frac{3\mathrm{P}^2}{8}\frac{\mathrm{k_p^c k_p^{\mu}}}{\pm\mathrm{L_r}}\frac{\hat{\mathrm{L}}_\mathrm{m}}{\hat{\mathrm{L}}_\mathrm{s}}\mathrm{V_s}sin(\bar{\Delta}_{\mathrm{sr}}),$$

$$c = -1 - \frac{3P^2}{8J}\frac{k_p^{\omega}\hat{L}_m}{\hat{L}_s}\lambda_{ds}\cos(\Delta\theta_{sr}),$$

$$d = -1 - \frac{3\mathrm{P}^2}{8\mathrm{J}}\frac{\mathrm{k_p^{\mu}\hat{L}_m}}{\hat{\mathrm{L}}_\mathrm{s}}\hat{\mathrm{a}}_{\mathrm{ds}}\sin(\bar{\Delta}_{\mathrm{sr}}),$$

$$e = -\frac{3\mathrm{P}^2}{8\mathrm{J}}\frac{\hat{\mathrm{L}}_\mathrm{m}}{\hat{\mathrm{L}}_\mathrm{s}}\hat{\mathrm{a}}_{\mathrm{ds}}\cos(\bar{\Delta}_{\mathrm{sr}}),$$

$$f = -\frac{3\mathrm{P}^2}{8\mathrm{J}}\frac{\hat{\mathrm{L}}_\mathrm{m}}{\hat{\mathrm{L}}_\mathrm{s}}\hat{\mathrm{a}}_{\mathrm{ds}}\sin(\bar{\Delta}_{\mathrm{sr}}),$$

$$g = -\mu_{sr} + \frac{\hat{\mu}_{sr}\pm\hat{L}_r}{\pm\mathrm{L_r}} + \frac{3}{2}\frac{\mathrm{k_p^c k_p^q}}{\pm\mathrm{L_r}}\frac{\hat{\mathrm{L}}_\mathrm{m}}{\hat{\mathrm{L}}_\mathrm{s}}\mathrm{V_s}sin(\bar{\Delta}_{\mathrm{sr}}),$$

$$h = -\frac{\mathrm{r_r} + \mathrm{k_p^c}}{\pm\mathrm{L_r}} - \frac{3}{2}\frac{\mathrm{k_p^c k_p^q}}{\pm\mathrm{L_r}}\frac{\hat{\mathrm{L}}_\mathrm{m}}{\hat{\mathrm{L}}_\mathrm{s}}V_s\cos(\bar{\Delta}_{\mathrm{sr}}),$$

$$i = -1 + \frac{3}{2}\frac{\mathrm{k_p^q\hat{L}_m}}{\hat{\mathrm{L}}_\mathrm{s}}V_s\sin(\bar{\Delta}_{\mathrm{sr}}),$$

$$j = -1 - \frac{3\mathrm{P}^2}{8\mathrm{J}}\frac{\mathrm{k_p^{\mu}\hat{L}_m}}{\hat{\mathrm{L}}_\mathrm{s}}\hat{\mathrm{a}}_{\mathrm{ds}}\cos(\bar{\Delta}_{\mathrm{sr}}),$$

$$k = \frac{3}{2}\frac{\hat{\mathrm{L}}_\mathrm{m}}{\hat{\mathrm{L}}_\mathrm{s}}V_s\sin(\bar{\Delta}_{\mathrm{sr}}),\ l = -\frac{3}{2}\frac{\hat{\mathrm{L}}_\mathrm{m}}{\hat{\mathrm{L}}_\mathrm{s}}V_s\cos(\bar{\Delta}_{\mathrm{sr}}),$$

$$m = \frac{k_i^c}{\pm L_r}, \text{ and } n = \frac{k_i^c k_i^{\mu}}{\pm L_r}.$$

III. STABILITY AND ANALYSIS FOR THE ENTIRE SYSTEM

The investigation in this paper is performed using the induction motor given in the Appendix. The approach adopted here is to observe the sensitivity of each parameter inaccuracies while holding other parameters constant. For example, in Fig. 4, the effect of the slip angle error on the real part of the system's eigenvalues is illustrated. There are three pairs of eigenvalues. The first pair $\hat{a}_{1,2}$ is related to speed and reactive power controllers, the second pair, $\hat{a}_{3,4}$ are related to the rotor current controller and the last pair $\hat{a}_{5,6}$ relates to the rotor current.

From the system matrix A^p, (17), it is clear that the stability of the system depends on the slip angle error $\bar{\Delta}_{sr}$. This is illustrated in Fig. 4(a) where the system becomes unstable at about $\bar{\Delta}_{sr} \approx 1.55\,rads$. Figs. 4(b) and 4(c) show that the eigenvalues $\hat{a}_{3,4}$ and $\hat{a}_{5,6}$ arte relatively stable as the slip angle increases. Fig. 5 (b) and (c) shows the dynamic response of the rotor currents to an error in the rotor speed lasting just about one cycle (60 Hz). Even though, the encoder resets and corrects the error after one cycle, the effect on the currents lasts much longer if not permanently.

IV. CONCLUSIONS

In this paper, the effect of rotor position error and machine parameter inaccuracies on a vector controlled DFIG turbine system has been analyzed. The results show that the error in rotor position has a significant effect on the stability of the entire system. It has been established that for a properly tuned controller gains, machine parameter inaccuracies do not affect the stability of the system but affects the placement of system poles in the left-hand plane.

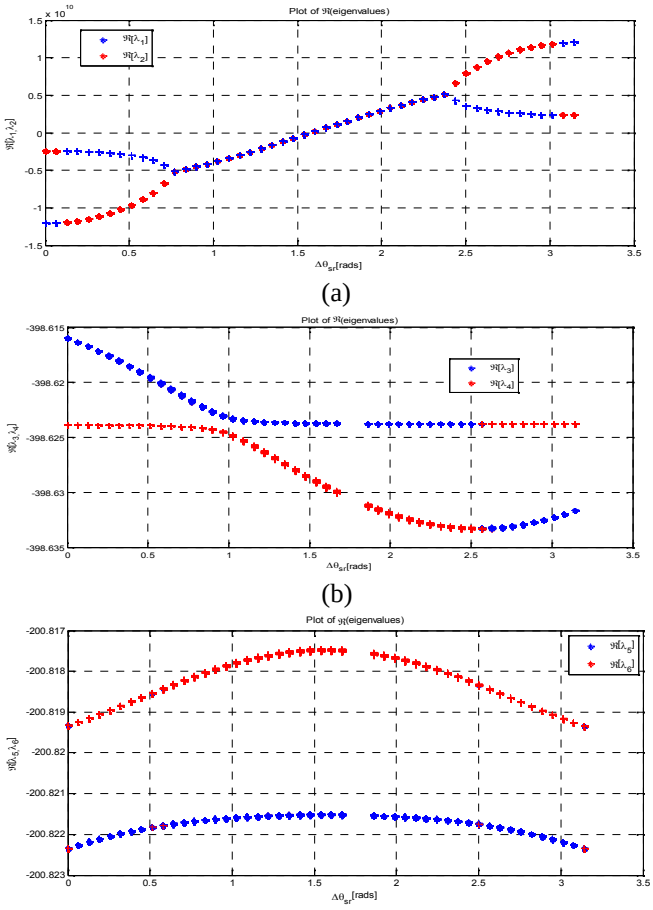

(a)

(b)

(c)

Figure. 4: contour lines of the real part of eigenvalues for (a) $^{a}_{1}$, (b) $^{a}_{3}$, and (c) $^{a}_{5}$ as a function of the slip angle error.

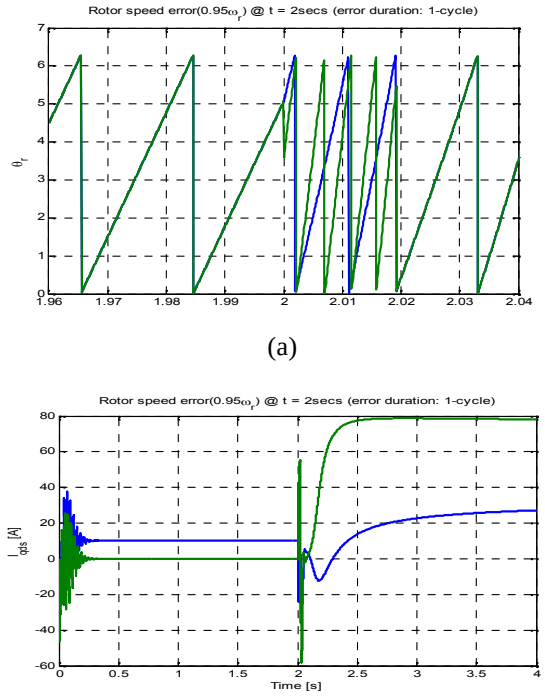

(a)

(b)

Figure 5: Effect of change slip angle on rotor *q-d* currents.

APPENDIX

5hp, 60Hz, 220–V line-line (rms), 6 pole wound–rotor induction motor

Stator resistance (r_s)	*0.65 Ω*
Rotor referred resistance (r_r)	*0.41 Ω*
Stator leakage inductance (L_{ls})	*2.6 mH*
Rotor referred leakage inductance (L_{lr})	*2.6 mH*
Magnetizing Inductance (L_m)	*0.0441 H*

REFERENCES

[1] T. Noguchi, H. Tomiki, S. Kondo, and I. Takahashi, "Direct power control of PWM converter without power-source voltage sensors," IEEE Transactions on Industry Applications, vol. 34, no. 3, pp. 473-479, May/June 1998.

[2] J. Arbi, M. J.-B Ghorbal, I. Slama-Belkhodja, and L. Charaabi, "Direct virtual torque control for doubly fed induction generator grid connection," *IEEE Transactions on Industrial Electronics*; vol. 56, no. 10, pp. 4163-4173, Oct. 2009.

[3] L. Xu and P. Cartwright, "Direct active and reactive power control of DFIG for wind energy generation," IEEE Transactions on Energy Conversion, vol. 21, no. 3, pp. 750–758, Sept. 2006.

[4] R. Pena, J. C. Clare and G. M. Asher "Doubly fed induction generator using back-to-back PWM converters and its application to variable-speed wind-energy generation," Proceedings. IEEE Power. Applications, vol. 143, no. 3, pp.231-341, May 1996.

[5] Z. Wang, G.-J Li, Y. Sun, and B. T. Ooi, "Effect of Erroneous Position Measurements in Vector-Controlled Doubly Fed Induction Generator," *IEEE Transactions on Energy Conversion*, vol. 25, no. 1, pp. 59-69,Mar. 2010.

[6] M. S. Carmeli, F. Castelli-Dezza, M. Iacchetti, and R. Perini , "Effects of Mismatched Parameters in MRAS Sensorless Doubly Fed Induction Machine Drives," *IEEE Transactions on Power Electronics* , vol. 25, no. 11, pp. 2842-2851, Nov. 2010.

[7] S. Bolognani, L. Peretti, and M. Zigliotto, "Parameter Sensitivity Analysis of an Improved Open-Loop Speed Estimate for Induction Motor Drives," IEEE Transactions on Power Electronics, vol. 23, no. 4, pp. 2127-2135 , Jul. 2008.

Kennedy Adinbo Aganah is an Assistant professor of electrical engineering at Tuskegee University. He received his B.S. in Mechanical Engineering from Kwame Nkrumah University of Science & Technology, Ghana in 2002. He received his M.S. and Ph.D., both in Electrical Engineering from Tuskegee University (2009), and Tennessee Tech University (2013), respectively. His research interests are in the areas of power electronics, smart grid, renewable energy systems, and distributed generation. He currently teaches Power Electronics, Power System Analysis, and Energy Conversion.